

The MICROMIXER: A Highly Linear Variant of the Gilbert Mixer Using a Bisymmetric Class-AB Input Stage

Barrie Gilbert, *Fellow, IEEE*

Abstract—This paper outlines the basic theory of a development of the Gilbert mixer. The bipolar junction transistor (BJT) differential pair widely used as the RF input stage is replaced by a bisymmetric Class-AB topology based on translinear principles. It does not have inherent gain compression, affording a greatly extended signal capacity. The linearity of variants of the basic form is excellent, providing two-tone intermodulation intercepts as high as +30 dBm, without the expenditure of high bias currents. It can operate on supplies as low as 2.2 V, with a power consumption of under 5 mW. The input impedance of this mixer is accurately controllable (typically 50 Ω) and provides a true broadband match. The noise figure depends on design details and is generally not as low as in mixers specifically optimized for noise performance, although acceptable for many receiver applications. Inductively degenerated variants can be tuned to a narrowband match at microwave frequencies and provide full-mixing SSB noise figures as low as 6.5 dB. Practical realizations are in use in applications to 1.9 GHz.

Index Terms— Active mixers, Class-AB RF cells, linear transconductance, microwave mixers, modulation.

I. INTRODUCTION

MIXERS have for decades played an indispensable role in communications systems as frequency-translation devices. At high microwave frequencies, rudimentary mixers based on a single diode are used. Below 1 GHz, discrete diode and FET-ring mixers, various single-transistor forms (bipolar, MOS, and GaAs), and dual-gate MOSFET types are very much in evidence. Systems integrated monolithically often use a topology called the *Gilbert mixer*,¹ which dates to the mid-1960's. Its RF input stage, usually a simple differential pair (sometimes using emitter degeneration in the bipolar case) sets fundamental limits to the attainable dynamic range. This and other limitations of the standard form are reviewed in Section II.

The small-signal linearity of this input stage, and thus the third-order intercept, can be greatly improved using several techniques, notably, the multi-tanh doublet and triplet [1]. However, the 1-dB gain compression point still falls short of

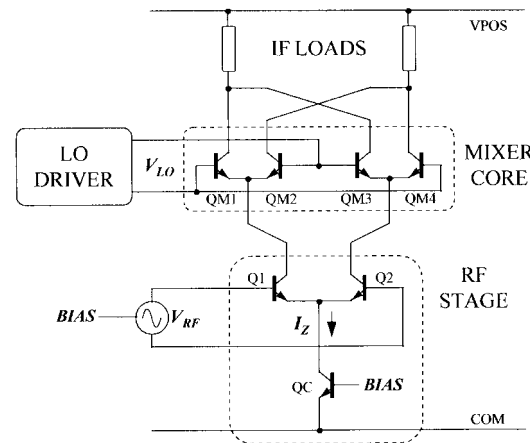


Fig. 1. Main elements of the standard form of the Gilbert mixer.

what may be required in handling large input signals without significant intermodulation. Further, these RF stages do not provide an accurate match to the source, even when using various types of impedance-transformation methods.

Accordingly, in Section III of this paper we present a basic topology, dubbed the MICROMIXER for reference purposes [2], [3]. It follows the general form of the Gilbert mixer, except for the use of a bisymmetric Class-AB RF stage. This provides a well-defined matching impedance and much lower input-related nonlinearity. There is no gain compression: rather, the gain increases at high input levels. Section IV presents ways to further improve the linearity and large-signal matching through the use of optimal resistive and inductive padding. These techniques provide exceptionally high intermodulation intercepts. This section also discusses suitable biasing means.

II. BACKGROUND

Fig. 1 shows the main elements of the *standard form* of a Gilbert mixer. The inherently balanced structure and the use of differential-mode signals is apparent. Mixers of this sort have been widely implemented in silicon IC's and more recently using GaAs MESFET's, SiGe or GaAs HBT's, or MOS devices. While this paper discusses silicon bipolar embodiments, it will be apparent that other technologies may be utilized, and in the case of SiGe HBT, with no modification to the theory.

Manuscript received February 25, 1997; revised May 1, 1997.

The author is with Analog Devices Inc., Beaverton, OR, 97006 USA.

Publisher Item Identifier S 0018-9200(97)05760-0.

¹Prior art by H. E. Jones was discovered following a patent application by the author for what is now called a Gilbert mixer, but that invention differed in several ways from the mixer shown in Fig. 1, having been developed as a "synchronous demodulator," and many of the claims dealt with its various auxiliary details. Nevertheless, credit must be given to Jones for having been the first to patent this basic form.

The actual mixing process—ideally, pure biphasic multiplication—is implemented in the current-steering cell, QM1–QM4, the *mixer core*. This is driven by V_{LO} , the differential-mode local oscillator (LO) voltage at its bases, typically about 100 mV in amplitude, which is arranged to have a suitable common-mode level. The IF output is produced at its collectors in differential current-mode form and is converted to a voltage at the IF load, whose impedance usually is chosen to provide maximum IF power consistent with the voltage swing range allowable at the collectors, with compression considerations in mind. Underneath this is the *RF stage*, comprising Q1 and Q2 biased by current-source QC. The RF voltage-mode signal is converted to differential current-mode form by this transconductance stage and presented to the common-emitter nodes of the mixer core. The noise and linearity of the RF stage are crucial to mixer performance. A useful aspect of this cell is that, in the absence of emitter degeneration, the bias current I_Z may be used to precisely control the conversion gain.

The focus of this paper will be on circuit cells that replace the Class-A (limited range) type of RF stage of the standard form with a Class-AB cell, which imposes basically no limitations on the maximum input amplitude. The combination of these RF input cells with the mixer core of the standard form has been named a MICROMIXER. Though our emphasis here is on the fundamentals, practical realizations will be constrained by the finite supply voltages (which, among other things, set a limit on the permissible IF swing), the limited current-handling capacity in the active devices (determined largely by the SPICE parameters IKF and RC), and the input compression levels of the following IF stage or second mixer.

A. Limitations of the Standard Form

The upper extent of the dynamic range is conventionally defined² by the 1 dB-compression point (usually expressed in power form, P_{1dB}), which bounds the mixer's capacity to cope with large signal amplitudes, while extrapolated intermodulation intercepts, notably, the two-tone third-harmonic intercept, I2P3, provide a basis for the calculation of the intermodulation in a complete signal chain. These metrics are notoriously misleading. Most modern RF stages do not conform to classical ideas about distortion, in particular, the notion that it is generated by an essentially *cubic* nonlinearity. Thus, the I2P3 is a function of the test level and may even improve at high input levels due to distortion cancellation. Further, the gain may actually increase again above the P_{1dB} point. The 1-dB compression point of the MICROMIXER will often be determined by limitations on the output (IF) signal-amplitude, rather than by the RF stage.

The input port of the mixer shown in Fig. 1 does not accurately match the source, since its impedance is fairly high and rather poorly controlled, being a function of the HF beta. On the other hand, the simpler grounded-base stage sometimes used in the singly-balanced mixer form, or a

differential grounded-base input (often driven via a balun) can provide input matching, which may be quite precise for small signals near the sensitivity limit.³ However, this match rapidly deteriorates for large signals, contributing to mismatch-related nonlinearity.

The lower reaches of the dynamic range are constrained by the input-referred wideband noise, usually expressed in terms of noise figure. This too can be a misleading indicator when input matching is imperfect. Additional noise due to the switching of the four-transistor core and spectrum folding (notably image noise) must also be considered. Though there are many distinctly different noise mechanisms, their separate identity is often lost in practical measurements. In the design of monolithic mixers, it is important to understand, and thereby control, these noise sources individually.

Mixer conversion gain is also an important parameter. This impacts the required noise and signal-handling performance of the subsequent first IF amplifier stage. The nonmixing (“amplifier-mode”) gain, exhibited when the mixer core is put into a simple “cascode” state by application of a large dc bias at the LO input, is determined by the ratio of the IF load impedance Z_{IF} to the input matching impedance Z_{IN} , and can be more rapidly determined in preliminary simulation studies than the mixing conversion gain, which will be approximately 4 dB ($\pi/2$) below the nonmixing gain, assuming that the core is operating in an essentially binary (sign-switching) fashion.

B. Signal Capacity of a BJT Pair

Consider the RF stage in Fig. 1. It is well known that the dc transfer characteristic of a simple bipolar junction transistor (BJT) differential pair is a hyperbolic tangent function. The voltage input V_{RF} may be expressed by the normalized variable $u = V_{RF}/2V_T$. The incremental gain is the derivative of the $\tanh(u)$ function, and has the form $G(u) = G_0 \operatorname{sech}^2(u)$, where G_0 is the peak gain, which occurs when $V_{RF} = 0$. $G(u)$ is 10% lower than G_0 for a dc input $V_{RF} \approx 17$ mV at a temperature⁴ of 300 K ($u = 0.327$). This characteristic voltage is proportional to absolute temperature (PTAT); to remind us of that, we will write the value as 17 mVP. Note that it does not depend on the bias current I_Z .

The third harmonic distortion, and thus the simple third-order intercept PH_3 can be found as follows. Let u represent the normalized amplitude $E/2V_T$ of a sinusoid RF input $E \sin \omega t$. Using a truncated power-series expansion for \tanh we can write

$$\begin{aligned} \tanh(u \sin \omega t) &\approx u \sin \omega t - (u \sin \omega t)^3/3 \dots \\ &= u(1 - u^2/4) \sin \omega t + (u^3/12) \sin 3\omega t. \end{aligned} \quad (1)$$

The output of the RF stage comprises a fundamental term of relative magnitude $H_1 = u(1 - u^2/4)$ and the third harmonic, $H_3 = u^3/12$. For a “test” input of $u = 0.01$ (that is, $E = 0.01 * 51.7$ mV = 517 μ V), $H_1 = 9.99975 \times 10^{-3}$,

³ Depending on the accuracy with which the bias current can be controlled, thus directly on the resistor technology.

⁴ In considering operation over a wide temperature range, it is important to remember that most mixer parameters (gain-compression point, intermodulation intercepts, noise figure, etc.) are fundamentally strong functions of temperature.

² Throughout this paper we will assume that these figures are referred to the *input* of the mixer, since this is where the fundamental nonlinearity arises for these structures; incidental compression may or may not occur at the IF load.

while $H_3 = 83.3 \times 10^{-9}$, which is 101.6 dB lower. Expressed as a power in 50 Ω , a sine amplitude of 517 μV corresponds to -55.7 dBm, so the PH₃ occurs at -4.9 dBm. An HD₃ of -40 dBc (1%) is generated by an input of about 18 mVP (-24.9 dBm re. 50 Ω).

We can determine the 1-dB compression point by setting $(1 - u^2/4) = 10^{-1/20}$, yielding $u = 0.66$. This corresponds to an amplitude of 34 mVP, or -19.35 dBm. Using a higher order expansion for the tanh function, we find $u = 0.718$, corresponding to an input of 37 mVP, or an input power of -18.6 dBm (the $P_{1\text{dB}}$) if the input were matched to 50 Ω . Of course, in the standard form of the Gilbert mixer, the Z_{IN} will be much higher. When the input is matched to the source (and this can only be approximate) through an impedance transformation, the P1 dB will be considerably lower.

C. Noise in the BJT Pair

In order to compare the fundamental noise performance of the MICROMIXER, we will further examine the RF stage of Fig. 1. For an ideal BJT, having no ohmic resistances, all the input noise would be generated by shot-noise processes. For the differential pair it is readily shown [1] that the collector noise currents $\sqrt{qI_Z}$ acting on the r_e 's of $2V_T/I_Z$ generate an equivalent voltage noise spectral density (NSD) of

$$E_{\text{SN}} = \frac{0.925 \text{ nV}/\sqrt{\text{Hz}}}{\sqrt{I_Z}} \quad \text{at } T = 300 \text{ K} \quad (2)$$

where I_Z is expressed in milliamps. Thus, the *short-circuit* input voltage noise of the BJT pair can be lowered in only one way: by increasing the bias current I_Z . There are two practical limits to how far the noise can be reduced by this means. First, there will often be constraints on power expenditure: to halve the noise voltage requires quadrupling the bias current. Second, above a certain value, another source of noise becomes troublesome, namely, that due to the base currents of Q1 and Q2 flowing in the source impedance, Z_S , which may itself be purely reactive, that is, noise-free.⁵

The ac base current noise for a single transistor operating at a collector current of I_C is $(\sqrt{2qI_C})/\beta(\omega)$, where $\beta(\omega)$ is beta of the transistor at some frequency of interest. The resulting voltage noise is therefore $(Z_S\sqrt{2qI_C})/\beta(\omega)$, which is seen to *increase* with the square-root of bias current. It is well known that for a given Z_S and $\beta(\omega)$ there will be an optimal value of I_C . The shot noise in the current-source transistor is not usually problematical, provided that the IF outputs are processed as a *differential* signal; this noise is common-mode and causes only an inconsequential modulation of the g_m . However, this noise becomes extremely troublesome when only one of the two IF outputs are used (single-sided loading). It can also be translated into the IF band by a strong blocking signal, sometimes posing a more important limitation to receiver sensitivity than intermodulation effects [6].

⁵If the source is a real resistance of, say, 50 Ω , the voltage noise induced by the base-current shot noise will calculate the same, but we then need to also include the resistor noise.

D. Emitter Degeneration

The linear range of the basic BJT differential pair in the RF stage is often extended by the addition of emitter degeneration resistors. These also introduce noise, so the question arises as to whether the overall dynamic range can be improved. A study of this issue [1] shows a theoretical improvement is possible, by an amount

$$20 \lg \frac{(1 + 1.7\sigma)}{\sqrt{(1 + 2\sigma)}} \text{ dB} \quad (3)$$

where $\sigma = I_Z R_E / 2V_T$ and R_E is the resistor added into each emitter. For example, let $\sigma = 10$ and $I_Z = 1$ mA, requiring $R_E = 517 \Omega$. The input-short-circuited noise spectral-density would be up from 0.925 nV/ $\sqrt{\text{Hz}}$ to 4.25 nV/ $\sqrt{\text{Hz}}$, a factor of 4.6, while the $V_{1\text{dB}}$ would be raised from 37 mVP to about 663 mVP, a factor of 18.

Thus, there is nearly a 12-dB improvement in dynamic range under these conditions. The effective input impedance of the RF stage is about $2\beta(\omega)(2R_E + 4V_T/I_Z)$, higher than before, making noise-matching even more difficult. The use of inductive degeneration is an obvious possibility in narrowband applications, without a noise penalty. Such also serves to transform the input impedance to an essentially resistive form, at frequencies where the ac beta is essentially f/f_T . Note, however, that the linear dependence of the g_m to the bias current of the RF stage in the standard form, useful in realizing variable-gain mixers, is invalidated by all forms of degeneration.

E. Multi-tanh Techniques

As noted earlier, the incremental g_m of a BJT differential pair varies considerably with the instantaneous voltage between the bases. Emitter degeneration reduces this dependence, but does not result in exactly constant incremental gain. A different linearizing technique uses the multi-tanh principle [1]. It can exhibit very low distortion for moderate signal amplitudes and provide an extended $V_{1\text{dB}}$ while the noise figure increases only slightly and the variable-gain capability is preserved. Only the briefest review is appropriate here.

The basic multi-tanh doublet uses two differential pairs, with opposing emitter-area ratios of A , which introduce an offset voltage⁶ of $\pm V_T \log A$. The offsets split the two tanh functions apart, and, with the correct choice of A , the resulting composite transfer function can exhibit a region close to $V_{\text{RF}} = 0$ over which the incremental gain is essentially flat, resulting in essentially zero distortion for moderate inputs. It has been shown [5] that this unique condition occurs for $A = 3.732$. The integer ratio 15 : 4 (3.75) is close, and may be a good choice, since a low-noise RF stage will probably use multistriple transistor geometries (15e and 4e) to achieve low values of r_{bb} . If we measure the dynamic range in terms of the ratio of the $V_{1\text{dB}}$ to the total input-referred noise-spectral density, we find that it is improved by nearly 5 dB for $A = 4$.

⁶These offset voltages can be introduced in several other ways, for example using input emitter-followers with or without emitter resistances and PTAT biases (see [1]), but this method is convenient in a monolithic context.

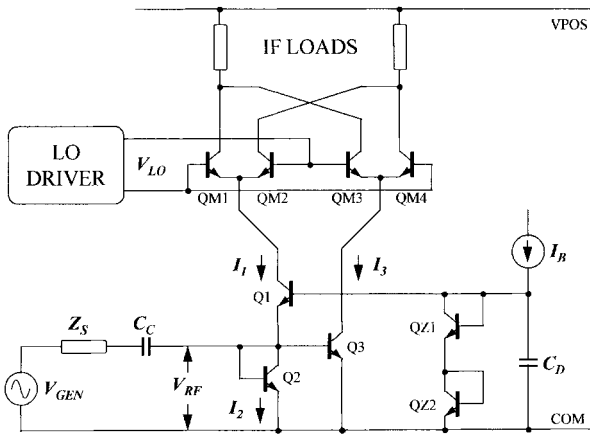


Fig. 2. The minimal MICROMIXER.

Many variants of the doublet have been used in mixer applications. For example, fixed- g_m realizations have been devised which combine the offset principle with emitter degeneration to achieve ultra-linear behavior. The idea can be extended to three (or more) pairs of transistors; the multi-tanh triplet is a very useful cell, providing further extension in the linear range. But the extension in V_{1dB} comes about only slowly with increasing complexity. Furthermore, none of these variants readily match to $50\ \Omega$ and require impedance transformation at their input.

III. THE BASIC MICROMIXER

The MICROMIXER uses a quite different approach to extending the linear range. The mixer core is identical to that of the standard Gilbert mixer. The important differences lie in the RF stage and the way it handles large signal amplitudes. Fig. 2 shows the circuit in its minimal form. Q1 can be viewed as a grounded-base stage. It delivers its output I_1 to the mixer pair QM1–QM2 in-phase. It can, *in principle*, handle unlimited amounts of current during large *negative* excursions of V_{GEN} . On the other hand, the current-mirror subcell Q2–Q3 can handle essentially unlimited amounts of current during *positive* excursions of V_{GEN} both at its input node and at its inverted-phase current output I_3 , which drives QM3–QM4. Acting together, these two subcells provide an overall transfer characteristic which is symmetrical to both positive and negative inputs, and which is *in principle* not limited by the choice of bias level. The differential current output $I_1 - I_3$ is linear with I_{RF} , although, as we shall see, the individual currents are quite nonlinear.

A. Biasing and Small-Signal Behavior

To assess the fundamental *shape* of the behavior, we will assume ideal transistors; greater realism can be added later, in progressive layers. Thus, at this point, we will conveniently ignore base currents. The adjunct branch comprising QZ1 and QZ2 is biased by I_B . The bias decoupling capacitor C_D provides a low-impedance ac ground for the base of Q1 and ensures that the HF bias noise is suppressed.

The translinear principle [4] states that, in a closed loop containing an equal number of clockwise-facing and counter-

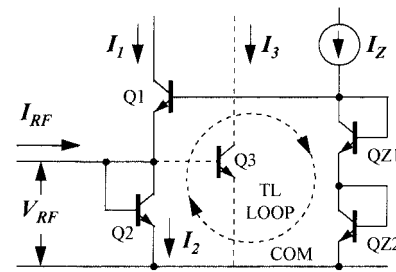


Fig. 3. Simplified input circuit.

clockwise-facing junctions, obeying an ideal exponential law, the product of the current-densities in each direction is equal. Applied to Fig. 2, we find that

$$I_Z^2/(A_1 A_2) = I_B^2/(A_{Z1} A_{Z2}) \quad (4)$$

where I_Z is the zero-signal bias current in Q1–Q3, and A_K is the emitter area of transistor Q_K . Fairly large transistors will be used for Q1–Q3 in order to minimize Johnson noise. If we assume their emitter area is M times that of QZ1 and QZ2, the quiescent bias in the RF stage will be simply $I_Z = M I_B$. The small-signal input resistance is the parallel sum of the r_e 's of Q1 and Q2, which are each V_T/I_Z . It follows that the incremental input resistance is

$$R_{IN} = \frac{V_T}{2I_Z}. \quad (5)$$

For a $50\text{-}\Omega$ input resistance, the unique value of $I_Z = 258.5\ \mu\text{A}$ must be used. Because of its pervasive importance, we will name this bias value I_{Z0} . To maintain a given R_{IN} over a wide temperature range, the bias currents should be PTAT, although closer analysis will show that some more subtle shaping should be used to compensate for such device parameters as dc beta and junction resistances. The bias will often be generated by a delta- V_{BE} cell and converted to a current by a resistor therein, whose temperature-coefficient immediately becomes that of R_{IN} .

The noise for the ideal case can be found by simply combining the shot-noise components in Q1–Q3. Expressed as a current, these are found to sum to

$$I_{SN} = \sqrt{(3/2)}\sqrt{2qI_Z} = \sqrt{3qI_Z}. \quad (6)$$

Assuming the source resistance R_S is matched directly by an equal incremental input resistance of R_{IN} given by (5), the total input noise voltage due to the input cell is

$$E_{SN} = 2R_{IN}I_{SN} = \frac{V_T}{I_Z}\sqrt{3qI_Z} = V_T\sqrt{(3q/I_Z)} \quad (7)$$

which evaluates to

$$E_{SN} = \frac{0.566\ \text{nV}/\sqrt{\text{Hz}}}{\sqrt{I_Z}} \quad \text{at } T = 300\ \text{K} \quad (8)$$

when I_Z is expressed in mA. For $I_Z = I_{Z0} = 258.5\ \mu\text{A}$, this amounts to $1.114\ \text{nV}/\sqrt{\text{Hz}}$, to which we must yet add the Johnson noise of the source, which is $0.912\ \text{nV}/\sqrt{\text{Hz}}$ for the $50\text{-}\Omega$ case, resulting in a total generator-referred noise of $1.44\ \text{nV}/\sqrt{\text{Hz}}$. This corresponds to a nonmixing noise figure of 3.96 dB, a value which is easily shown to be independent

of the choice of R_{IN} , provided the matching condition is preserved. However, since the distortion will be a function of some *absolute* peak voltage, that is, a certain number of units of V_T , it follows that the choice of a reduced R_{IN} , say, 25 Ω , resulting in a higher input *power* for a given voltage, will result in a higher dynamic range. In practice, maintaining a broadband R_{IN} of less than 50 Ω will often be difficult at high frequencies due to packaging considerations.

B. Large-Signal Behavior

We can begin an exploration of the large signal behavior of this cell by considering first its response to a pure current drive I_{RF} applied to the input node. Fig. 3 shows the main translinear loop⁷ embracing Q1, Q2, QZ1, and QZ2. To simplify this analysis, without any loss of generality, we can assume that all transistors are the same size and the primary bias current is now I_Z . In general, the input current will cause the collector current of Q1 to assume some value $I_1 \neq I_Z$, while I_2 must be simply $I_1 + I_{RF}$.

Applying the translinear principle to this loop, we have

$$I_Z I_Z = I_1 I_2 = I_1 (I_1 + I_{RF}). \quad (9)$$

The solution can be expressed most compactly by defining a modulation factor $\lambda = I_{RF}/2I_Z$. We find

$$I_1 = I_Z \{\sqrt{(\lambda^2 + 1) - \lambda}\} \quad (10a)$$

$$I_2 = I_Z \{\sqrt{(\lambda^2 + 1) + \lambda}\}. \quad (10b)$$

Note that λ may be of either polarity and is not in principle bounded by the value of I_Z . These currents are individually nonlinear, as must be the case for any Class-AB circuit. However, provided that the current mirror section (Q2–Q3 in Fig. 2) is linear, and assuming otherwise ideal devices, the differential drive to the mixer core is

$$I_1 - I_3 = 2\lambda I_Z = I_{RF}. \quad (11)$$

The voltage at the RF input node is

$$\begin{aligned} V_{RF} &= V_{BEZ} + V_T \log(I_{C2}/I_Z) \\ &= V_{BEZ} + V_T \log\{\sqrt{(\lambda^2 + 1) + \lambda}\} \\ &= V_{BEZ} + V_T \sinh^{-1} \lambda \end{aligned} \quad (12)$$

where V_{BEZ} is the base-emitter voltage at the quiescent current I_Z . It follows that the large-signal incremental input resistance is

$$R_{IN}(\lambda) = \frac{V_T}{2I_Z} \frac{1}{\sqrt{(\lambda^2 + 1)}}. \quad (13)$$

This predicts that for a signal current I_{RF} equal in magnitude to three times the quiescent bias, R_{IN} will be only 10% of its zero-signal value. The analysis becomes transcendental as soon as the source resistance is included, in seeking to determine

⁷It is interesting to note that this four-junction loop is identical to that found in a simple translinear multiplier cell, in vector arithmetic circuits, as the input stage of a common current-conveyor topology (using complementary devices), and even in the Class AB output stage found in numerous op-amp designs.

how R_{IN} depends on the *generator voltage* V_{GEN} . A fairly accurate approximation for this case is

$$R_{IN} = \frac{V_T}{2I_Z} \frac{1}{\sqrt{\{(\gamma/4)^4 + (\gamma/2)^2 + 1\}}} \quad (14)$$

where $\gamma = V_{GEN}/V_T$, to within $\pm 2.4\%$ of the zero-signal value $R_{IN,0}$. For example, the incremental input resistance drops to 13% of $R_{IN,0}$ for an instantaneous input voltage of either +250 mV or –250 mV at the generator ($\gamma = 9.67$ at $T = 300$ K).

Other aspects of the MICROMIXER can be studied and developed more efficiently through the use of simulation. This can, of course, be as easily performed using comprehensive device models, operating at “realistic” signal frequencies, and can include all package parasitics and numerous other practical complications. But our first objective remains to explore the *basic personality* of these cells, and it will be instructive, for the present, to continue to use highly idealized translinear models.⁸

C. Swept- V_{GEN} Exploration

For the simulation studies, the high side of V_{GEN} is coupled directly to the input node via a source resistance R_S (that is, C_C is shorted) and the bias voltage at node B is buffered by an ideal voltage-follower to which the “low” side of V_{GEN} is connected. Provided that the easy condition $A_1 A_{Z1} = A_2 A_{Z2}$ is met, the voltage at B will be equal to that at the mixer’s input node when $V_{GEN} = 0$. A further detail is important in noise studies, namely, that node B , as well as the primary base node, must be well-decoupled by a grounded capacitor. Using this temporary artifice of a dc-coupled signal path, we can probe the incremental values of important circuit variables as a function of the instantaneous value of the RF voltage, V_{GEN} , which here refers to the dc (perturbation) value to which is added a zero-amplitude ac component.

Experimental techniques of this sort can generate valuable insights by exploring the large-signal properties of an RF cell. Here, V_{GEN} was swept while observing the incremental ac gain and input resistance and input-referred noise. The mixer core was “hung” in an extreme drive state ($V_{LO} = 200$ mV dc). The IF loading circuit was given an effective transimpedance of 100 Ω using noise-free resistors (Z -elements) of low value followed by an ideal differential-to-single-sided converter; this interim test scheme avoids compression at the IF load, which can be studied separately.

Fig. 4 shows some typical results using an arbitrary test frequency of 300 MHz. The incremental gain increases with the magnitude of V_{GEN} since for either polarity of input swing, the r_e of either Q1 or Q2 decreases. As noted above, at very high RF drive levels the incremental R_{IN} becomes asymptotic to zero, as either I_1 or I_2 becomes very high. Consequently, the incremental gain increases asymptotically toward +6 dB, suggesting that *this RF stage will not exhibit gain compression*, but rather an *expansion* in the main-carrier output at high drive levels. This is one of several unusual aspects of the

⁸This method of layered discovery and development, particularly well-suited to bipolar technologies, has been named *Foundation Design* by the author.

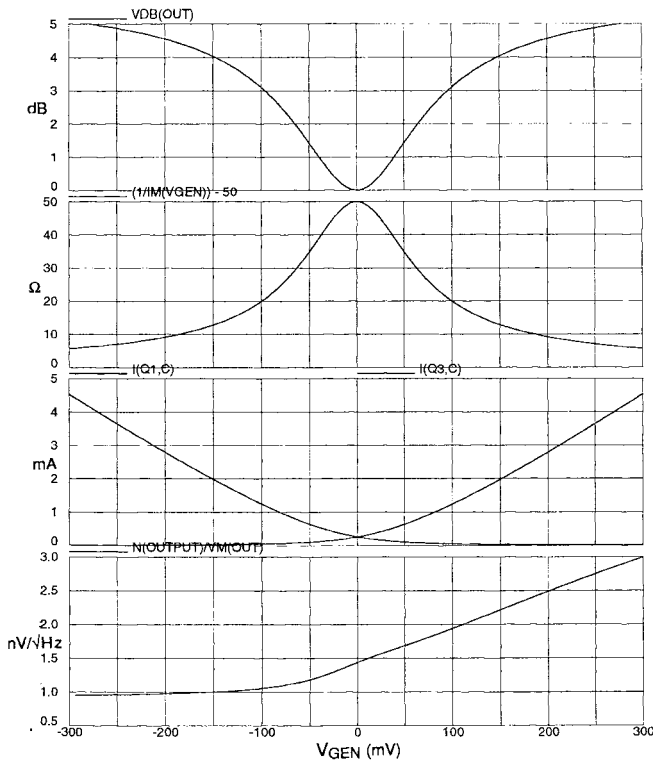


Fig. 4. Swept- V_{GEN} results for basic cell. Top to bottom: incremental gain; incremental R_{IN} ; collector currents of Q_1 , Q_3 ; input-referred noise.

MICROMIXER. The input-referred NSD for $V_{\text{GEN}} = 0$ is $1.44 \text{ nV}/\sqrt{\text{Hz}}$, as predicted by the first-order theory, but it varies asymmetrically with V_{GEN} for reasons given later. Relative to the noise of $R_S = 50 \text{ } \Omega$ ($0.912 \text{ nV}/\sqrt{\text{Hz}}$), the amplifier-mode noise figure evaluates to $20 \lg(1.44/0.921) = 3.96 \text{ dB}$. Operating as a mixer,⁹ folding and harmonic noise will raise the single sideband (SSB) noise figure to about 8 dB.

D. Distortion of the MICROMIXER

Fig. 4 also shows the currents I_1 and I_3 . Their individual nonlinearity is apparent. When driven at very high input levels *only one* of the two outputs will be active at any time (that is, during the polarity reversals of the RF input). These signal components recombine in-phase at the IF output, after each has traversed *one half* of the mixer core. We need to consider how this might impact the overall mixer integrity.¹⁰ It was shown above that the signal of importance—the algebraic difference in these two currents—is linear with respect to the input current I_{RF} . Thus, the signal distortion (for the idealized case) will be almost entirely due to the nonlinearity between V_{GEN} and I_{RF} . It is for this reason that the greatest attention is given in this paper to the linearity of R_{IN} .

We have already found that the voltage generated at the input V_{RF} can be expressed with reference to the fixed voltage

⁹Neglecting the additional noise due to the switching action in the mixer core; see [1] for an analysis.

¹⁰Note in passing that the widely used singly balanced mixer, having an RF stage that is simply a grounded-base or grounded-emitter transistor, is not only very nonlinear but is completely missing one signal polarity in its output at very high drive levels.

V_B as

$$V_{\text{RF}} = V_B + V_T \sinh^{-1} \lambda \quad (12a)$$

where $\lambda = I_{\text{RF}}/2I_Z$. To determine the input nonlinearity, we can reverse cause and effect and calculate the value of V_{GEN} needed to cause a current I_{RF} , as follows:

$$\begin{aligned} V'_{\text{GEN}} &= I_{\text{RF}}R_S + V_T \sinh^{-1} \lambda \\ &= I_{\text{RF}}R_S + V_T \{ \lambda + \lambda^3/6 + (3/40)\lambda^5 \dots \} \\ &\approx I_{\text{RF}}R_S + V_T \lambda + V_T \lambda^3/6 \dots \end{aligned} \quad (15)$$

Now taking λ to have a sinusoidal waveform, and noting that for the matched condition $R_S = R_{\text{IN}} = V_T/2I_Z$, we find

$$V'_{\text{GEN}}/V_T = \{ 2\lambda - (\lambda^3/8) \} \sin \omega t + (\lambda^3/24) \sin 3\omega t. \quad (16)$$

The ratio of the third harmonic to the fundamental in V'_{GEN} , that is, the third harmonic distortion HD3, is thus approximately $\gamma^2/48$.

To a close approximation, the peak value of I_{RF} for a $-30 \text{ dBm}/50 \text{ } \Omega$ input is $\pm 200 \text{ } \mu\text{A}$. Thus, at $T = 300 \text{ K}$, when $I_Z = I_{Z0} = 258.5 \text{ } \mu\text{A}$, the peak value of λ is 0.387, and the theoretical HD3, which has not taken into account the many other distortion effects that will arise at high frequencies, evaluates to 3.1×10^{-3} , or -50.1 dBc , from which we can estimate that the simple third-harmonic intercept PH3 will be at about $-30 + (50.1/2) = -4.95 \text{ dBm}/50 \text{ } \Omega$.

E. Large-Signal Measurements

Classical approaches to RF design and circuit analysis are based on the assumption that the active device parameters remain constant throughout the signal cycle; the perturbations in operating point caused by the signal are ignored. This assumption allows one to use small-signal modeling concepts, such as S -parameters. In practice, however, this naïve assumption is not valid in *any* mixer, which is inherently very nonlinear when treated in its entirety. In a Class-AB input structure, the “stable parameter” assumption is even less true. The intrinsic device speed when driven to low currents will be degraded, leading to nonlinear phase effects, which may result in a failure of the signal fragments to add correctly at the IF output. However, though clearly of concern, all mixers suffer from such large-signal aberrations. Thus, in the simple Class-A RF stage of the Fig. 1 mixer, Q_1 and Q_2 undergo a significant modulation in their dynamic parameters at high input levels. Using modern low-inertia devices at signal frequencies well below their maximum performance capabilities, these dynamic nonlinearities are often tolerable.

Fig. 5 shows what we will call the *harmonic signature* for the basic MICROMIXER,¹¹ for a single-tone 300 MHz input ranging from -30 dBm to $+15 \text{ dBm}$, re. $50 \text{ } \Omega$. The top panel shows the difference between the actual value (H_1) and the extrapolated value (EH_1) of the fundamental output on an expanded scale. As predicted from the swept- V_{GEN} results, it becomes too high for increasing input levels. At very high levels, where the average R_{IN} over each cycle drops to almost

¹¹The small amount of incidental second-harmonic distortion has been omitted from these results for reasons of clarity.

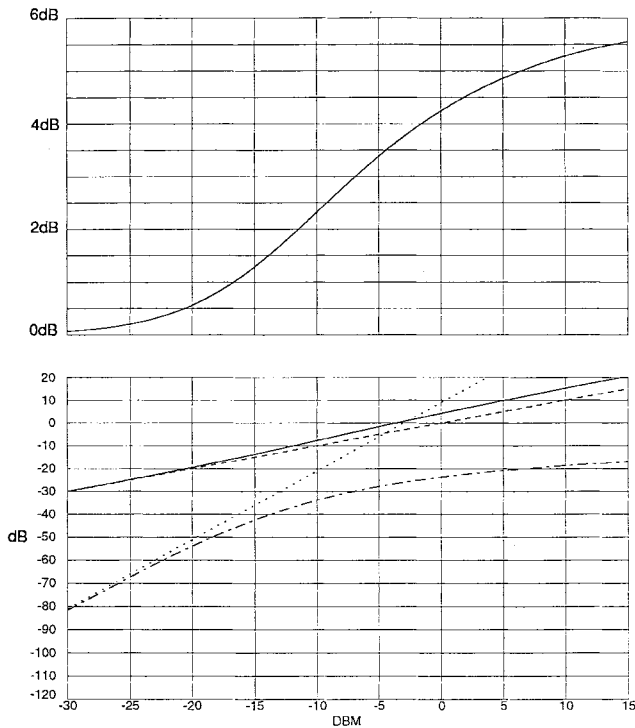


Fig. 5. The harmonic signature for the minimal MICROMIXER ($I_Z = 258.5 \mu\text{A}$). Top panel: Gain error of fundamental; bottom panel: fundamental, actual HD3, and extrapolations.

zero, the incremental gain doubles. It follows that we cannot define a $P_{1\text{dB}}$, unless we stretch the definition to mean a 1 dB gain *error* (either high *or* low), in which case, it occurs at -13 dBm .

The third harmonic component H_3 is well below the extrapolated line EH_3 , and its magnitude relative to the fundamental actually *decreases* at high inputs. The simple third-harmonic intercept PH_3 is at -4.5 dBm , extrapolating from the -30 dBm level, where H_3 is -51 dBc . It is shown in [1] that, assuming a cubic nonlinearity, the input-referred two-tone third-order intermodulation intercept I2P3 is 4.8 dB below the single-tone intercept PH_3 . This is a useful rule-of-thumb, allowing shorter simulation times in preliminary evaluations. Here, the predicted I2P3 is -9.3 dBm ; however, actual two-tone measurements on Si and SiGe MICROMIXERS show considerably better values, for example, -3.7 dBm at 1.8 GHz.

As noted, the incremental input *resistance* R_{IN} of the MICROMIXER can be set to 50Ω , or to higher or lower values by appropriate choice of bias current, and drops to very low values at large positive or negative excursions of the input voltage. In practice, the inertial aspects of the transistor will affect the input impedance Z_{IN} at frequencies above about 5% of the f_T of the transistor. Just as importantly, the package parasitics will play a major role in determining the actual input impedance in, say, L-Band operation. Attention must be given to the two loops involving a) input node \rightarrow base of $Q_1 \rightarrow C_D \rightarrow$ ground return and b) input node \rightarrow emitters of Q_2 and $Q_3 \rightarrow$ ground return.

These are well-known practical aspects of layout and packaging for microwave circuits, and it is assumed that whatever the final topology of the mixer, such issues need to be ad-

ressed in the development of a practical device. Accordingly, we will remain focused for the rest of this paper on improving the *intrinsic* behavior of the circuit, without a strong concern for the limitations of a particular IC technology.

IV. IMPROVEMENTS TO THE MICROMIXER

A further extension in signal linearity can be obtained by improvements to the linearity of the intrinsic R_{IN} and/or the use of resistively- or inductively-padded schemes. The modified noise performance and practical biasing methods will be described. An obvious way to stabilize R_{IN} would be to use a larger bias current (thus lowering the r_e 's) and then pad up the input resistance using a series resistor. Though clearly not optimal from a noise perspective, this solution is pointing in the right direction; it also lowers the inherent nonlinearity in each of the currents.

Reasoning that the r_e of either Q_1 or Q_2 diminishes for large inputs while the opposite r_e gets very high, two padding resistors R_P , each of 50Ω (assuming that is still our target R_{IN}) can be placed in each emitter, as shown in Fig. 6. Having done that, we now must operate the transistors at $I_Z = 517 \mu\text{AP}$, so that $(r_e + R_P)/2 = 50 \Omega$. Clearly, this will not result in a constant R_{IN} , but we can be sure that it will be precisely 50Ω for arbitrarily large positive or negative values of V_{GEN} as well as for $V_{\text{GEN}} = 0$. The current mirror can now be converted to an emitter-degenerated form, which improves its accuracy and reduces the effect of shot noise. These resistors introduce a bias drop of $I_Z R_P$ (here, one V_T), and we need to add corresponding resistors in the bias branch.

The simulation results of Fig. 7 show that R_{IN} is 50Ω for $V_{\text{GEN}} = 0$ and is again asymptotic to 50Ω for very large instantaneous inputs ($\pm 1 \text{ V}$), but it now peaks to 60.13Ω at $\pm 210 \text{ mV}$. Such a modulation of R_{IN} is probably not catastrophic, though as we shall see very shortly, better solutions can readily be found. The gain now dips *down* by -0.83 dB (compare this to the *increase* seen in the minimal MICROMIXER) at this same value of V_{GEN} before creeping back up to 0 dB at very large inputs (rather than to $+6 \text{ dB}$). This intriguing result suggests that there may be some intermediate padding arrangement which exhibits even more constant input impedance and gain over moderate ranges of V_{GEN} . The total input-referred zero-signal noise, including the resistive source $R_S = 50 \Omega$, is up to about $1.64 \text{ nV}/\sqrt{\text{Hz}}$, so the amplifier-mode noise figure is 5.1 dB .

The harmonic signature for this case (Fig. 8) has some interesting artifacts. First, the gain at the fundamental frequency never drops below 0.55 dB of the ideal extrapolation, and at high inputs it is asymptotic to 0 dB . Once again, there is no 1-dB compression point, but neither is there any gain expansion. Second, the H_3 is lower than for the minimal MICROMIXER, resulting in a higher PH_3 of $+7 \text{ dBm}$; the high-level H_3 is well below the extrapolation, so this figure may give a somewhat pessimistic view of the performance. There is a deep notch in H_3 close to 0 dBm .

A value of 50Ω was used for R_P in conjunction with a bias current of $I_Z = 2I_{Z0} = 517 \mu\text{AP}$, since we could

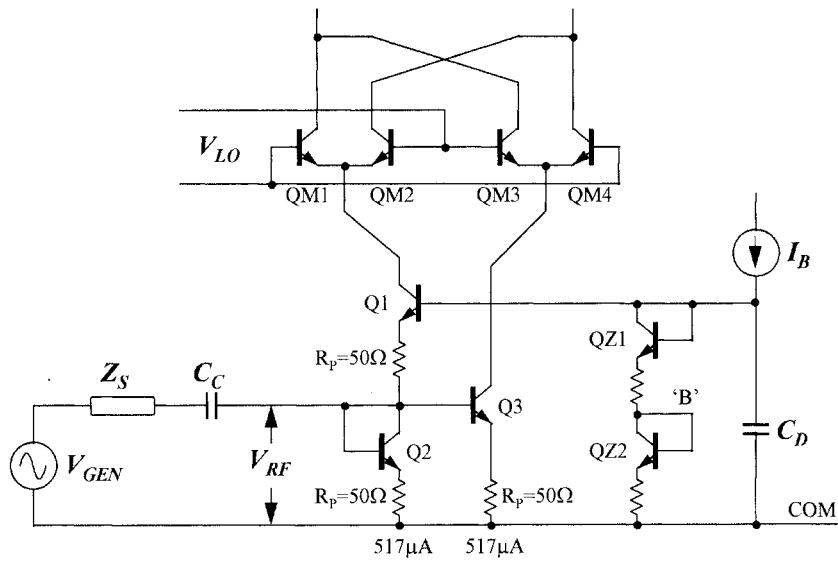


Fig. 6. Input impedance padded by addition of emitter resistors.

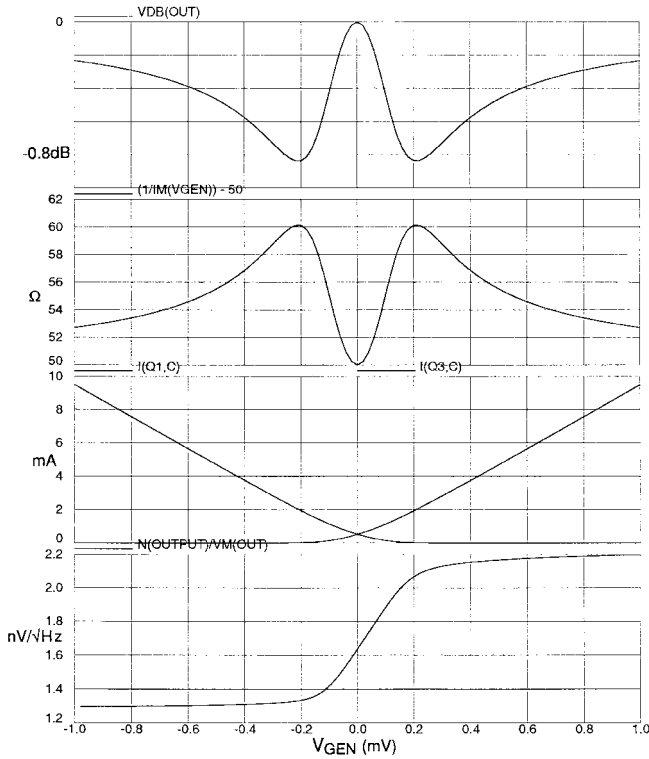


Fig. 7. Swept- V_{GEN} results for 50- Ω -padded MICROMIXER ($I_Z = 517 \mu A$). Compare with Fig. 4.

foresee that would result in the net R_{IN} at high drives being asymptotic to 50 Ω . But a moment's reflection shows that a *higher* value of R_P could be used, up to nearly 100 Ω for a 50- Ω match, by increasing I_Z above $2I_{Z0}$. Within the range $50\Omega \leq R_P \leq 100 \Omega$, the higher bias currents might actually be useful in extending the bandwidth when using large (low- $r_{bb'}$) transistors. However, the higher bias currents require larger voltage drops across these resistors, which will eventually impact the minimum permissible supply voltage, and the noise figure worsens.

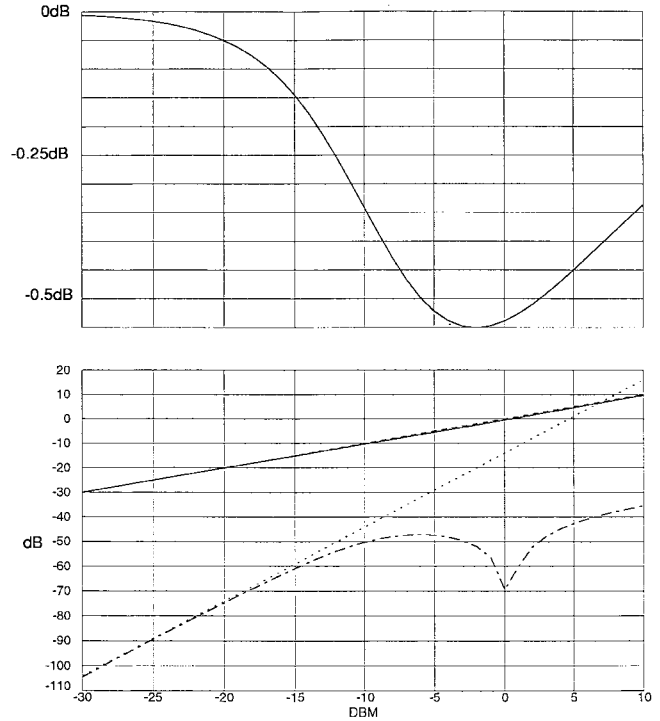


Fig. 8. Harmonic signature for the 50- Ω -padded MICROMIXER ($I_Z = 517 \mu A$). Top panel: gain error of fundamental; bottom panel: fundamental, actual HD3, and extrapolation.

A. The Optimal MICROMIXER

We will now explore the alternative option, namely, to choose R_P inside the range 0 to 50 Ω , using an I_Z in the range I_{Z0} to $2I_{Z0}$ (258.5–517 μA). It is easily shown that the derivative of the input resistance is uniquely zero (that is, conversion from the generator voltage to the signal current is perfectly linear) when a simple condition is met, namely

$$I_Z = \frac{3 V_T}{4 R_{IN}} \quad (17)$$

at which point the bias drop across each resistor is $V_T/2$.

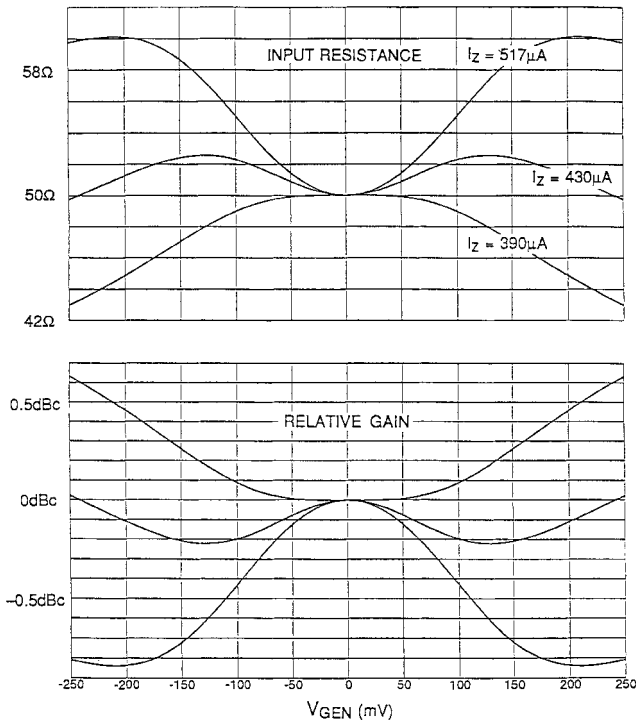


Fig. 9. Incremental gain and R_{IN} for various other padding conditions.

Thus for a 50- Ω input, this optimal solution occurs at $I_Z = 1.5I_{Z0} = 387.75 \mu\text{AP}$ and $R_P = 33.33 \Omega$. In practice, slightly higher bias levels will result in a useful improvement in large-signal linearity.

Fig. 9 shows the incremental R_{IN} for $I_Z = 390 \mu\text{AP}$ ($R_P = 34 \Omega$) and $430 \mu\text{AP}$ ($R_P = 40 \Omega$) over the range $-250 \text{ mV} \leq V_{\text{GEN}} \leq +250 \text{ mV}$, which for a sinusoidal input would correspond to a loaded input power of -8 dBm ; the previous result is also shown for comparison. The small-signal linearity is near-optimal using $I_Z = 390 \mu\text{AP}$, while it remains flatter over more of this input range when using $I_Z = 430 \mu\text{AP}$ (maximum deviation of $+2.5 \Omega$). Note that the incremental gain follows a predictable inverse relationship to the sum of R_S and R_{IN} . For $I_Z = 430 \mu\text{AP}$, it varies by 0.22 dB over this input range, and by only 0.003 dB over $-50 \text{ mV} \leq V_{\text{GEN}} \leq +50 \text{ mV}$ for $I_Z = 390 \mu\text{AP}$.

The harmonic signature for $I_Z = 390 \mu\text{AP}$ is shown in Fig. 10. Again there is no 1 dB gain compression point; instead, the gain increases to $+1.2 \text{ dB}$ at $+15 \text{ dBm}$ and is 0.57 dB high at 0 dBm . The H_3 is extremely low, being -98 dBc at -22 dBm , resulting in a PH_3 of $+27 \text{ dBm}$. An unwelcome artifact of this response is that over the signal range -22 dBm to $+7.5 \text{ dBm}$ the H_3 now lies above the extrapolated line. Fig. 11 shows the results for $I_Z = 430 \mu\text{AP}$. The fundamental output is even more constant, dropping by only -0.12 dB at -9 dBm and rising to $+0.63 \text{ dB}$ at $+15 \text{ dBm}$. The H_3 remains very low, now -78 dBc at -30 dBm , resulting in a PH_3 of $+9 \text{ dBm}$. Furthermore, now both the H_2 (not shown) and H_3 always remain below the extrapolations, and the H_3 is notably lower than for the last case at high signal levels, being only -42 dBc at an input power of $+15 \text{ dBm}$.

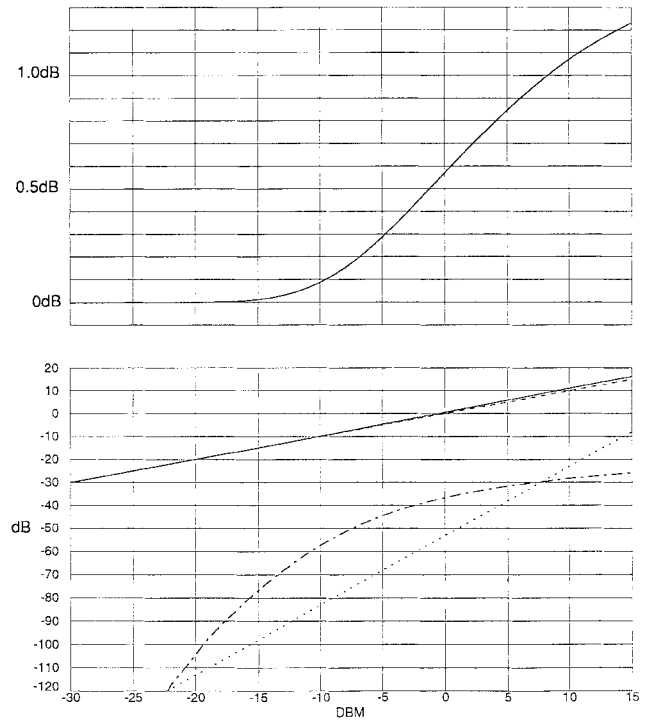


Fig. 10. Harmonic signature $I_Z = 390 \mu\text{AP}$, $R_P = 34 \Omega$. Top panel: gain error of fundamental; bottom panel: fundamental, actual HD3, and extrapolation.

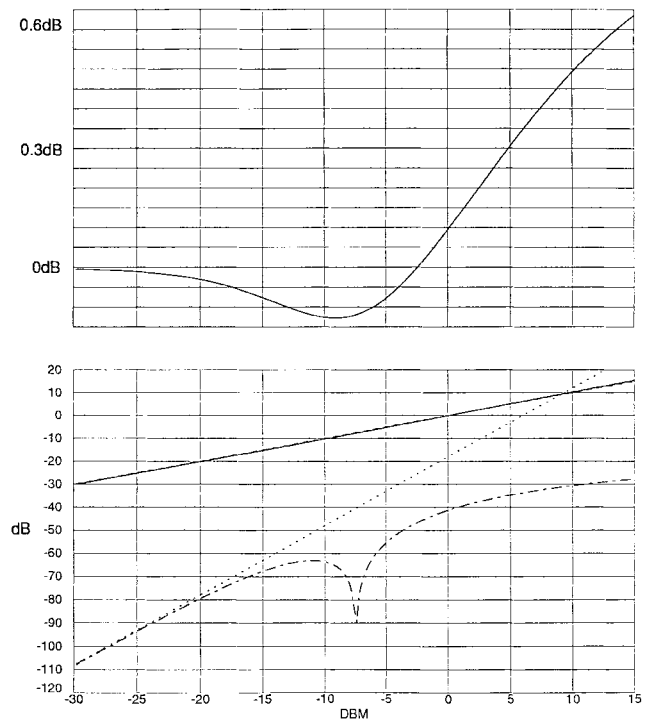
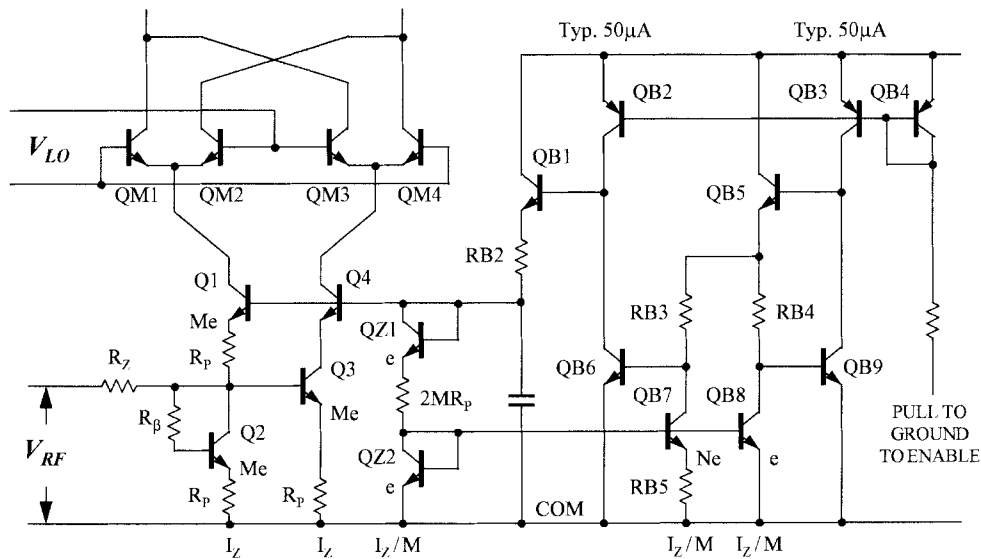


Fig. 11. Harmonic signature $I_Z = 430 \mu\text{AP}$, $R_P = 40 \Omega$. Top panel: gain error of fundamental; bottom panel: fundamental, actual HD3, and extrapolation.

Numerous simulation studies have been carried out to explore the intermodulation properties of this cell using a two-tone test input. Using the "optimal" bias of $390 \mu\text{AP}$, test tones of 320 MHz and 340 MHz and a transistor with a TF of

Fig. 12. The T -padded form and bias details.

10 ps ($f_T = 16$ GHz) the side-tone powers using test levels of -30 dBm are -92.8 dB below the wanted signals; I2P3 thus evaluates to $-30 + (92.8/2) = 16.5$ dBm. As always, caution is needed in interpreting results based on simplified simulations, which nevertheless usefully serve to *bound* the best-possible performance.

The variation of input noise as a function of the bias current has been explored over a wide range using an algorithmic value of $R_F = 2R_{IN} - V_T/I_Z$. For the $50\text{-}\Omega$ case, a useful approximation for the total noise spectral density, referred to the generator, including that of the source resistance, real resistors for R_F , and collector shot noise, but excluding base resistance or base shot noise, is

$$E_N = \left\{ 1 + \frac{2}{9}(1 - \exp \xi) + \frac{1}{24} \left(1 - \exp \frac{\xi}{24} \right) \right\} \times 1.44 \text{ nV}/\sqrt{\text{Hz}} \quad (18)$$

where $\xi = (I_Z - I_{Z0})/I_{Z0}$. The value is within ± 0.02 nV/ $\sqrt{\text{Hz}}$ for all bias currents above I_{Z0} .

B. The Tee-Padded MICROMIXER

A further refinement to the design results when the padding scheme just described is augmented with a series-connected input resistor. The left-hand side of Fig. 12 shows this simple modification. The addition of R_Z alters the required value of R_P . Having chosen R_Z , considerable latitude remains in the choice of I_Z . Thus, the optimization space is rather large. The cascode Q4 is added to equalize the V_{CE} of Q2 and Q3; it also reduces the amount of LO voltage appearing at the emitters of QM3 and QM4 that couples back to the input. In practice, however, the incidental inequality of V_{CE} may help to recover some of the current gain in the mirror lost by reason of its finite ac beta, and the cascode may be contraindicated.

The approach used in studying this circuit has been to choose combinations that result in a null in the derivative $\partial G/\partial V_{GEN}$ at $V_{GEN} = 0$, that is, in flat gain versus instantaneous input voltage for small signals. Table I lists some

TABLE I

R_Z Ω	R_P Ω	I_Z μAP	PH ₃ dBm (-30dBm)	I2P3 dBm (-30dBm)	SSB NF dB	R_{IN} Ω ($V_{RF} = \pm 100\text{mV}$)	ΔG dB
0	33.33	388	16.3	15.5	9.64	49.00	0.088
2	32.14	405	16.7	16.6	9.75	49.23	0.067
4	30.71	422	17.4	17.0	9.87	49.31	0.060
6	29.35	441	18.0	17.5	10.00	49.42	0.051
8	28	462	18.6	18.2	10.14	49.52	0.042
10	26.67	485	19.3	18.8	10.30	49.61	0.034
15	23.33	554	21.1	20.6	10.75	49.80	0.020
20	20	647	23.3	22.4	11.25	49.90	0.008
25	16.67	776	24.5	25.3	11.90	49.95	0.004
30	13.33	970	27.1	28.5	12.75	49.98	0.001

combinations and various performance criteria. In all cases an input match to $50\ \Omega$ (and thus a 0-dB relative gain) at $V_{GEN} = 0$ is provided. The I2P3 was determined for test signals of 320 MHz and 340 MHz, each of either -30 dBm (± 10 mV at the RF input) or -10 dBm (± 100 mV), in this particular case using a transistor having an effective f_T of 16 GHz.

From the point of view of realizability and robustness, we are especially interested in solutions resulting in resistor combinations that are integer multiples of a unit element. One in particular stands out, namely, $I_Z = 647\ \mu\text{AP}$, $R_Z = R_P = 20\ \Omega$. For this case, R_{IN} varies from $50\ \Omega$ at $V_{GEN} = 0$ and falls only slightly to $49.9\ \Omega$ at $V_{GEN} = \pm 200$ mV ($V_{RF} = \pm 100$ mV); the gain theoretically varies by only 0.008 dB. This points toward very linear performance as a mixer, as evidenced by the excellent two-tone (320/340 MHz) results. The noise figure in SSB full-mixing mode is a moderate 11.25 dB.

A practical biasing system is also shown on the right of Fig. 12. It is based on an all-NPN delta- V_{BE} (PTAT) cell [7] tightly integrated into the RF stage, resulting in precise biasing. In an optimal realization, all resistors would be thin-film, having good absolute accuracy and near-zero temperature-coefficient, for excellent control of R_{IN} . The core of this cell is

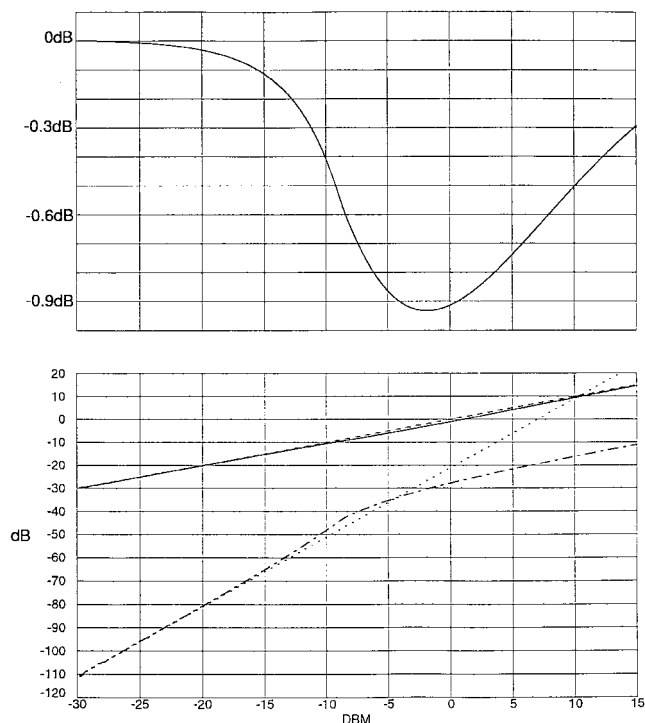


Fig. 14. Harmonic signature for the L-band variant ($I_Z = 1.18$ mA). Top panel: gain error of fundamental; bottom panel: fundamental, actual HD3, and extrapolation.

beyond the primary objective of this paper, which has been to outline the general conceptual and theoretical framework of the MICROMIXER and point to some new areas for development.

V. CONCLUSION

The MICROMIXER topology provides an accurate input impedance, high intermodulation intercepts, and an almost unlimited signal capacity at its input, arising from the use of a Class-AB topology, while maintaining acceptable noise performance. This paper has provided a brief overview of its potential. The results are based largely on simple models of the devices, in order to better compare the variants on a similar basis, without the coloration introduced by complex dynamic effects, and as an aid to the development of insights leading to improved topologies. It is clear that if the fundamentals are not right, there is little benefit in proceeding to the later steps of adding the greater realism captured in the full transistor model.

Nonetheless, for modern low-inertia transistors (that is, having few-picosecond transit times and few-femtofarad capacitances) operating at sensible bias currents, the “low frequency” predictions are reliable out to many hundreds of megahertz and still useful as a comparative tool in the microwave range. In practice, package parasitics, biasing-current errors, and instrumentation issues will have a much greater impact on determining mixer performance at microwave frequencies, provided that due care is taken in the design and layout of the monolithic circuit.

The MICROMIXER is not a panacea. More recent developments in active mixers—along quite different lines—provide considerably lower noise figures while still maintaining excellent linearity and variable gain, to be reported at a future time. Its chief attraction lies in the very high intercepts that can be achieved, making the topology of potential value in transmit modulators and other high-level applications. However, at microwave frequencies the use of on-chip inductive degeneration allows these benefits to be preserved while lowering the noise figure back into a range appropriate for receiver applications.

ACKNOWLEDGMENT

The author gratefully acknowledges the work of G. Dawe in implementing these concepts in a practical monolithic context and R. Simonson for his careful measurements on early versions of the mixer. The useful comments of the reviewers have also been noted.

REFERENCES

- [1] B. Gilbert, “Design considerations for active BJT mixers,” in *Low-power HF Microelectronics; A Unified Approach*, G. Machado, Ed. London: IEE, ch. 23, pp. 837–927, 1996.
- [2] G. Dawe, J.-M. Mourant, and A. P. Brokaw, “A 2.7 V DECT RF transceiver with integrated VCO,” in *ISSCC Dig. Tech. Papers*, Feb. 1997, pp. 308–309.
- [3] B. Gilbert, “Design considerations for BJT active mixers,” BCTM 1996 Short Course.
- [4] ———, “Current-mode circuits from a translinear viewpoint: A tutorial,” in *Analogue IC Design: The Current-Mode Approach*, C. Toumazou, F. J. Lidgley, and D. G. Haigh, Eds. London: IEE, ch. 2, pp. 11–91, 1990.
- [5] ———, “IF amplifiers for monolithic bipolar communications systems,” presented at EPFL Electronics Laboratories Advanced Engineering Course on RF Design for Wireless Communications Systems, Lausanne, July 1–5, 1996.
- [6] R. G. Meyer and A. K. Wong, “Blocking and desensitization in RF amplifiers,” *IEEE J. Solid-State Circuits*, vol. 30, pp. 944–946, Aug. 1995.
- [7] B. Gilbert, “Monolithic voltage and current references: Theme and variations,” in *Analog Circuit Design*, H. Huisjing, R. van de Plassche, and W. Sansen, Eds. Norwell, MA: Kluwer, pt. III, pp. 269–352, 1996.



Barrie Gilbert (M’62–SM’71–F’84) was born in 1937 in Bournemouth, England.

He pursued an early interest in solid-state devices at Mullard Ltd., working on first-generation planar IC’s. Emigrating to the United States in 1964, he joined Tektronix, Beaverton, OR, where he developed the first electronic knob-readout system and other advances in instrumentation. Between 1970–1972 he was Group Leader at Plessey Research Laboratories. He joined Analog Devices Inc., Beaverton, OR, in 1972 and was appointed as ADI

Fellow in 1979. He manages the development of communications IC’s at the NW Labs in Beaverton.

For work on merged logic Dr. Gilbert received the IEEE “Outstanding Achievement Award” (1970) and the IEEE Solid-State Circuits Council “Outstanding Development Award” (1986). He was Oregon Researcher of the Year in 1990 and received the Solid-State Circuits Award (1992) for “Contributions to Nonlinear Signal Processing.” He has five times received the ISSCC Outstanding Paper Award and has been issued over 40 patents. He holds an Honorary Doctorate from Oregon State University.